Energy Conversion and Management 52 (2011) 641–647

Contents lists available at ScienceDirect

Energy Conversion and Management

journal homepage: www.elsevier.com/locate/enconman

An automotive thermoelectric–photovoltaic hybrid energy system using maximum power point tracking

Xiaodong Zhang *, K.T. Chau

Department of Electrical and Electronic Engineering, The University of Hong Kong, Pokfulam Road, Hong Kong

ARTICLE INFO

Article history:
Received 10 September 2009
Received in revised form 15 March 2010
Accepted 18 July 2010
Available online 16 August 2010

Keywords:
Automotive
Hybrid system
Maximum power point tracking
Thermoelectric
Photovoltaic
Power conditioning

ABSTRACT

In recent years, there has been active research on exhaust gas waste heat energy recovery for automobiles. Meanwhile, the use of solar energy is also proposed to promote on-board renewable energy and hence to improve their fuel economy. In this paper, a new thermoelectric–photovoltaic (TE–PV) hybrid energy system is proposed and implemented for automobiles. The key is to newly develop the power conditioning circuit using maximum power point tracking so that the output power of the proposed TE–PV hybrid energy system can be maximized. An experimental system is prototyped and tested to verify the validity of the proposed system.

1. Introduction

With ever increasing oil consumption and growing concern on environmental protection, there is a pressing need to develop green energy sources for automobiles, including the waste heat energy recovery system and solar energy system [1,2]. These kinds of energy sources can be used to online feed various automotive electronics or charge the battery for storage, hence reducing the oil consumption and the carbon emission of the automobiles.

Nowadays, the fuel efficiency of the internal combustion engines (ICEs) employed in the gasoline vehicles, diesel vehicles and hybrid electric vehicles (HEVs) is only around 25%, whereas about 40% is lost in the form of the waste heat of exhaust gas. It is reported that the fuel economy of ICEs can be increased by up to 20% simply by converting about 10% of the waste heat to electricity [3]. Consequently, the waste heat energy recovery technology has been actively investigated, such as the Rankine cycle system [4] and the thermoelectric (TE) system [5]. Compared with the Rankine cycle system, the TE system has the advantages of maintenance free, silent operation, high reliability, and involving no moving and complex mechanical parts [6]. On the other hand, the use of photovoltaic (PV) technology has been proposed for HEVs so as to promote the concept of on-board renewable energy and hence to further improve their fuel economy [2].

The concept of energy hybridization has been accepted for EVs and HEVs [7–9]. Compared with individual energy sources, the hybrid energy system can offer some definite advantages for automobiles, namely the higher fuel economy due to the increase of on-board renewable energy, the better energy security due to the use of multiple resources, and the higher control flexibility due to the coordination for charging the same pack of batteries. So, the TE–PV hybrid energy system is promising for all kinds of automobiles propelled by ICEs.

So far, only a few TE–PV hybrid energy systems have been proposed. In [10], the TE generator (TEG) is affixed to the rear of the PV generator (PVG) to decrease its temperature because the lower temperature can improve the efficiency of the PVG. So, the TEG simply functions to improve the solar energy conversion efficiency. In [11], the TEG and PVG are integrated in a mobile computing system to potentially extend the battery life. However, its output power is too low for automotive electronics. In [12], the TEG and PVG are integrated to back up each other for better energy security. However, these configurations can not be directly used for automobiles. In [13], the TEG and PVG are combined to form a hybrid energy system for HEVs. It employs the SEPIC–SEPIC converter to perform the maximum power point tracking (MPPT). However, this multiple input converter (MIC) has shortcomings for practical implementation.

In this paper, a new TE–PV hybrid energy system with the Ćuk–Ćuk MIC is proposed and implemented. The keys of this hybrid energy system are to harvest the waste heat energy of the ICE by the TEG so as to improve the fuel economy, and to convert the solar

* Corresponding author. Tel.: +852 28578617; fax: +852 25598738.
E-mail address: xiaodong@eee.hku.hk (X. Zhang).

0196-8904/$ - see front matter © 2010 Elsevier Ltd. All rights reserved.
doi:10.1016/j.enconman.2010.07.041

energy by the PVG so as to utilize the on-board renewable energy. Compared with the SEPIC–SEPIC MIC [13], the Ćuk–Ćuk MIC can offer non-pulsating input current and output current, which can significantly minimize the disturbance on system operation, and potentially enhance the battery life [5]. Furthermore, the Ćuk–Ćuk MIC needs three inductors while the SEPIC–SEPIC MIC needs four inductors, leading to lower cost, lighter weight and smaller volume.

In Section 2, the system configuration of the proposed TE–PV hybrid energy system will be described. Section 3 will be devoted to presenting the design and implementation of the proposed power conditioning system (PCS) with the MPPT controller. In Section 4, detailed experimental results will be given to verify the validity of the proposed hybrid energy system. Finally, a conclusion will be drawn in Section 5.

2. System configuration

Fig. 1 shows the system configuration of the proposed TE–PV hybrid energy system for automotive application. This hybrid system is composed of a TEG branch, a PVG branch, a MPPT controller, a Ćuk–Ćuk MIC, and a battery. In practice, the MPPT controller measures the output voltages and currents of the TEG and PVG, respectively, and generates the switching signals to the Ćuk–Ćuk MIC according to the MPPT algorithm. The controller also monitors the terminal voltage and body temperature of the battery. In case of overvoltage or overheat, the MIC is switched off to protect the battery.

The TEG is used to harvest the waste heat of the exhaust gas from the ICE. There are two main accessible waste heat sources, namely the radiator system and the exhaust gas system [14]. The radiator system functions to pump the coolant through the chambers in the heat engine block so as to absorb the excess heat and draw it away, hence avoiding the engine block overheating and seizure. On the other hand, the exhaust gas system functions to emit the flue gas which occurs as a result of the combustion of fuels in the ICE. Currently, the TEG is mostly installed in the exhaust gas system because this configuration is easy to be implemented and has less influence on the operation of the engine. According to the temperature distribution of the exhaust gas system, a proper TE material can readily be determined [15]. Also, the cooling system of the TEG can share with the engine cooling loop to further increase the output power [16].

For the PVG, the PV panels can be installed on the vehicle roof. In general, the vehicle roof area that can accommodate the PV panels ranges from about 1.5 m^2 for a passenger car to about 30 m^2 for a bus. So, by connecting a proper number of PV panels in series and in parallel, the PVG is able to provide the desired voltage and current ratings for the proposed system.

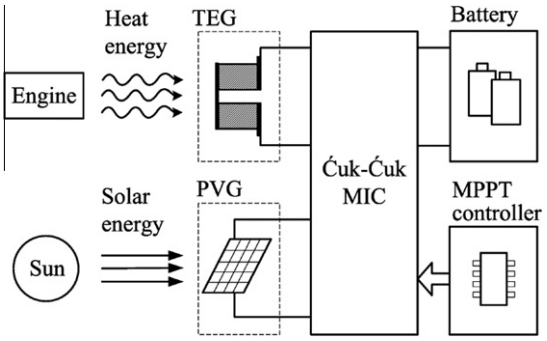

Fig. 1. Proposed TE–PV hybrid energy system.

In this paper, the TE–PV hybrid energy system is used to charge the battery. When the battery voltage is lower than a preset minimum value $V_{bat,min}$, and the input voltage of the TEG or PVG branch is higher than the corresponding minimum value $V_{TE,min}$ or $V_{PV,min}$, the charging process is activated. When the maximum voltage $V_{bat,max}$ is reached, the battery is regarded as fully charged.

3. Proposed power conditioning system

3.1. MPPT

Since the output power characteristics of the TEG are highly nonlinear and heavily depend on the heat source, cooling system and external load, a proper power conditioning circuit and MPPT control are required. Similarly, the PVG output power characteristics heavily depend on the irradiance, ambient temperature and external load. So, it also needs a proper power conditioning circuit and MPPT control. By using the Thevenin transformation, the equivalent circuit of the TEG and PVG can separately be represented by a DC voltage source in series with an internal resistance [17]. As shown in Fig. 2, the power conditioning circuit functions to track the maximum power point of the TEG or PVG. By tuning the duty cycle of its PWM switching signal to enable the input resistance $r_i = V_i/I_i$ equal to the internal resistance of the energy source r_g, the MPPT can be performed. In the TE–PV hybrid energy system, the MIC circuit must be able to handle these two energy sources and realize their MPPT individually or simultaneously.

3.2. Ćuk–Ćuk MIC

The Ćuk converter shown in Fig. 3 is selected for power conditioning of the TEG and PVG. First, the output voltage of the TEG or PVG may widely and dynamically vary with external physical factors. The Ćuk converter having both step-up and step-down characteristics can handle a wide range of input voltage variation caused by different temperature differences and insolation levels. Second, when the switch is turned off, the Ćuk converter can inherently block the DC input from the TEG or PVG energy sources to the load due to the existence of the intermediate capacitor. Third, both of the input current and output current of the Ćuk circuit are non-pulsating. By properly winding the input and output inductors on the same core, the ripple amplitude can be reduced to zero. This merit can significantly minimize the disturbance on the TEG or PVG operating points, and potentially enhance the battery life. Based on the synthesizing principles of the MIC [18], two Ćuk circuits are lumped together to form a Ćuk–Ćuk MIC as shown in Fig. 4. This MIC not only retains the merits of the Ćuk circuit, but also enables the TEG and PVG delivering the power to the load individually or simultaneously.

The Ćuk converter can be operated in three modes: continuous current mode (CCM), discontinuous inductor current mode (DICM), and discontinuous capacitor voltage mode (DCVM). Generally, the CCM is more suitable for high voltage, high current input application; the DICM is for high voltage, low current input application; and the DCVM is for low voltage, high current input application.

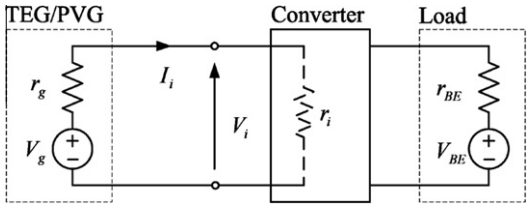

Fig. 2. MPPT using power conditioning circuit.

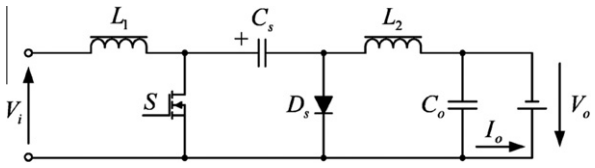

Fig. 3. Basic Ćuk converter.

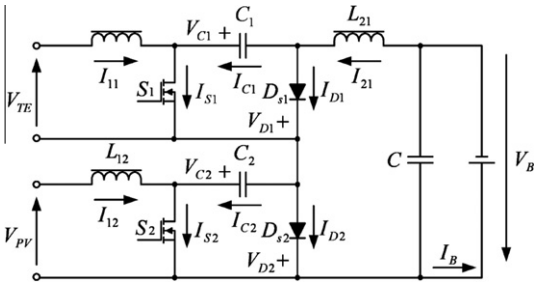

Fig. 4. Proposed Ćuk–Ćuk MIC.

Since the TEG and PVG are of low output voltage, hence low input voltage for the Ćuk–Ćuk MIC, it is preferred to operate in the DCVM mode.

When the two input inductors L_{11}, L_{12}, the output inductor L_{21} and the output capacitor C are large enough to guarantee that the inductor currents I_{11}, I_{12}, I_{21} and the output voltage V_B are constant, the topological stages and key waveforms of the Ćuk–Ćuk MIC charging the battery in the DCVM are depicted in Figs. 5 and 6, respectively.

According to the key waveforms, the capacitor voltage V_{C1} and diode voltage V_{D1} for the TEG branch can be expressed as:

$$V_{C1} = \begin{cases} \frac{I_{11}(1-D_1)T_s}{C_1} - \frac{I_{21}t}{C_1}, & 0 < t < d_1T_s \\ 0, & d_1T_s < t < D_1T_s \\ \frac{I_{11}(t-D_1T_s)}{C_1}, & D_1T_s < t < T_s \end{cases} \quad (1)$$

$$V_{D1} = \begin{cases} V_{C1}, & 0 < t < d_1T_s \\ 0, & d_1T_s < t < T_s \end{cases} \quad (2)$$

where D_1 is the duty cycle of the switch S_1, T_s is the switching period, and d_1 is the duty cycle of the diode D_{s1}. At the steady state, the average voltages of L_{11} and L_{21} equal zero. From Eqs. (1) and (2), the input voltage can be written as:

$$V_{TE} = \overline{V_{C1} - V_{D1}} = \frac{1}{T_s}\int_{d_1T_s}^{T_s} V_{C1}dt = \frac{T_sI_{11}(1-D_1)^2}{2C_1} \quad (3)$$

Therefore, the input resistance of this TEG branch in the DCVM is given by:

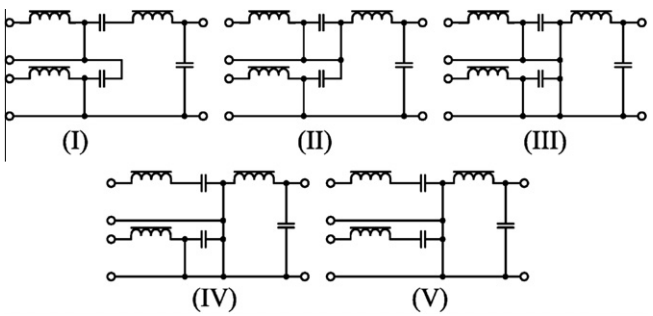

Fig. 5. Topological stages in DCVM.

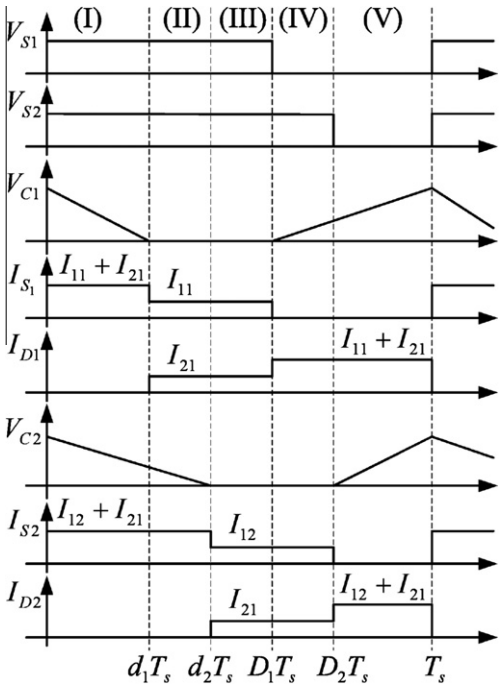

Fig. 6. Key waveforms in DCVM.

$$r_{TE} = \frac{V_{TE}}{I_{11}} = \frac{T_s}{2C_1}(1-D_1)^2 \quad (4)$$

Similarly, the capacitor voltage V_{C2} and diode voltage V_{D2} for the PVG branch can be expressed as:

$$V_{C2} = \begin{cases} \frac{I_{12}(1-D_2)T_s}{C_2} - \frac{I_{21}t}{C_2}, & 0 < t < d_2T_s \\ 0, & d_2T_s < t < D_2T_s \\ \frac{I_{12}(t-D_2T_s)}{C_2}, & D_2T_s < t < T_s \end{cases} \quad (5)$$

$$V_{D2} = \begin{cases} V_{C2}, & 0 < t < d_2T_s \\ 0, & d_2T_s < t < T_s \end{cases} \quad (6)$$

where D_2 is the duty cycle of the switch S_2, and d_2 is the duty cycle of the diode D_{s2}. Consequently, the input resistance of this PVG branch in the DCVM can be obtained from Eqs. (5) and (6):

$$r_{PV} = \frac{V_{PV}}{I_{12}} = \frac{T_s}{2C_2}(1-D_2)^2 \quad (7)$$

As indicated in Eqs. (4) and (7), when the inductors and output capacitor of the MIC are sufficiently large, the input resistance of each branch does not associated with the load. It indicates that it can perform the MPPT the same as a basic Ćuk circuit provided that the two branches of the MIC are both in the DCVM. By calculating the ampere–second balance across C_1 and C_2, it yields:

$$I_{11}(1-D_1) = I_{21}d_1 \quad (8)$$

$$I_{12}(1-D_2) = I_{21}d_2 \quad (9)$$

Then, by using the input power balance equation of $V_{TE}I_{11} + V_{PV}I_{12} = V_BI_{21}$ with $I_{21} = (V_B - V_{BE})/r_{BE}$ as depicted in Fig. 2, d_1 and d_2 can be deduced from Eqs. (8) and (9) as:

$$d_1 = \frac{KI_{11}(1-D_1)}{2P_{in}} \quad (10)$$

$$d_2 = \frac{KI_{12}(1-D_2)}{2P_{in}} \quad (11)$$

where $K = V_B + \sqrt{V_B^2 + 4P_{in}r_{BE}}$ and P_{in} is the input power of both the TEG and PVG branches. Obviously, the DCVM can be ensured if

$D_1 \geqslant d_1$ and $D_2 \geqslant d_2$. From Eqs. (10) and (11), the criteria for the Ćuk–Ćuk MIC to ensure the DCVM can be deduced as:

$$\frac{KI_{11}}{2P_{in}} \leqslant \frac{D_1}{1-D_1} \tag{12}$$

$$\frac{KI_{12}}{2P_{in}} \leqslant \frac{D_2}{1-D_2} \tag{13}$$

3.3. Implementation

The proposed TE–PV hybrid energy system with the MPPT control is implemented as shown in Fig. 7. The TEG is composed of 18 pieces of TE modules (Model TEP1-12656-0.6), an induction heater, and a heatsink. These modules are connected with six pieces electrically in series and three branches in parallel. On the other hand, the PVG is composed of nine pieces of polycrystalline–silicon PV panels (Model SR10-36), and tungsten halogen lamps. These PV panels are connected electrically in parallel. A 12 V 38 Ah lead-acid battery is selected as the battery load, which has an internal resistance of 7.5 mΩ. The prototype of the whole system is shown in Fig. 7a.

At the beginning of the experiment, the output characteristics of the TEG and PVG are measured at specific working conditions by changing the external load. Based on the measured characteristics of the TEG and PVG, the circuit components of the proposed Ćuk–Ćuk MIC can be designed. The switching frequency is set as 100 kHz. The microcontroller chip DSP2812 operates at 30 MHz clock frequency, incorporating with 16 12-bit ADC channels, 18 k 16-bit SRAM, and 16 PWM channels in two Event Managers. So, it can provide fast computing speed, precise A/D conversion, and user-friendly programmable PWM generation. Thus, it is adopted as the MPPT controller. The detailed PCS is shown in Fig. 7b.

Although different MPPT methods have been proposed, the perturb-and-observe (PAO) method is still the most common one in practice due to its simplicity and system independence. Thus, the proposed MIC adopts this method to perform the MPPT for both the TEG and PVG branches of the hybrid energy systems. Basically, the PAO method is an iterative self-searching approach, which can be described by following expression:

$$D_{k+1} = \Delta D_{k+1} + D_k$$

$$\Delta D_{k+1} = \mathrm{sgn}(P_k - P_{k-1})\Delta D_k$$

where D_i and P_i are the switching signal duty cycle and the input power of the MIC branch at the sampling instant i, respectively, and ΔD_i is initialized as 0.5%, $i = 1, 2, \ldots, k, k+1, \ldots$.

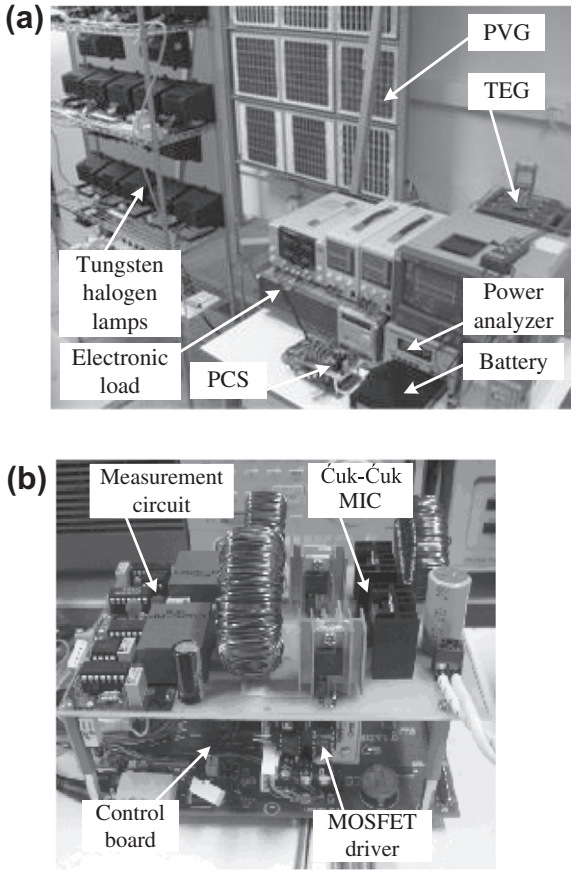

Fig. 7. System prototype. (a) Whole system and (b) PCS.

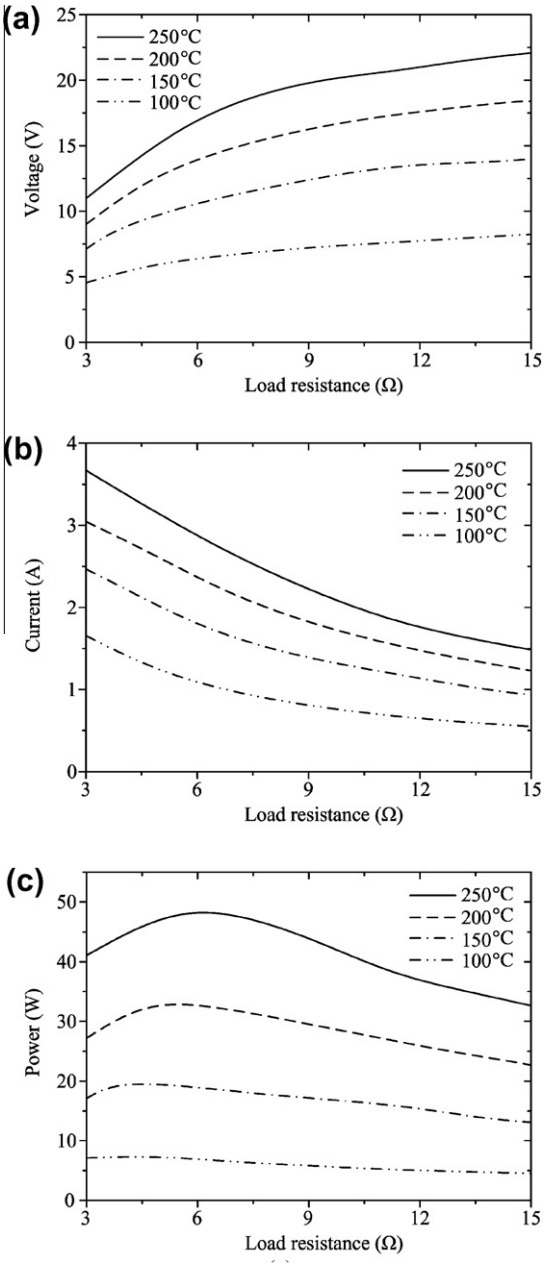

Fig. 8. Output characteristics versus load resistance of the TEG. (a) Output voltage. (b) Output current. (c) Output power.

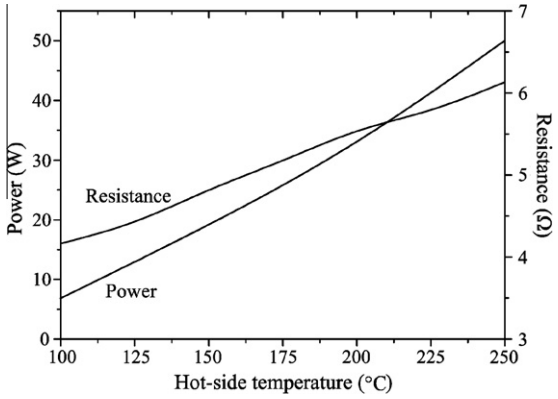

Fig. 9. Output power and internal resistance of the TEG.

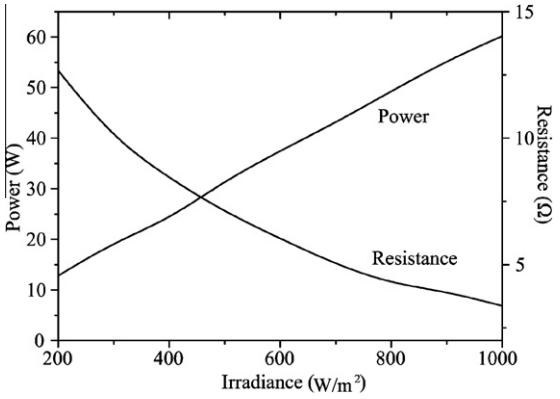

Fig. 11. Output power and internal resistance of the PVG.

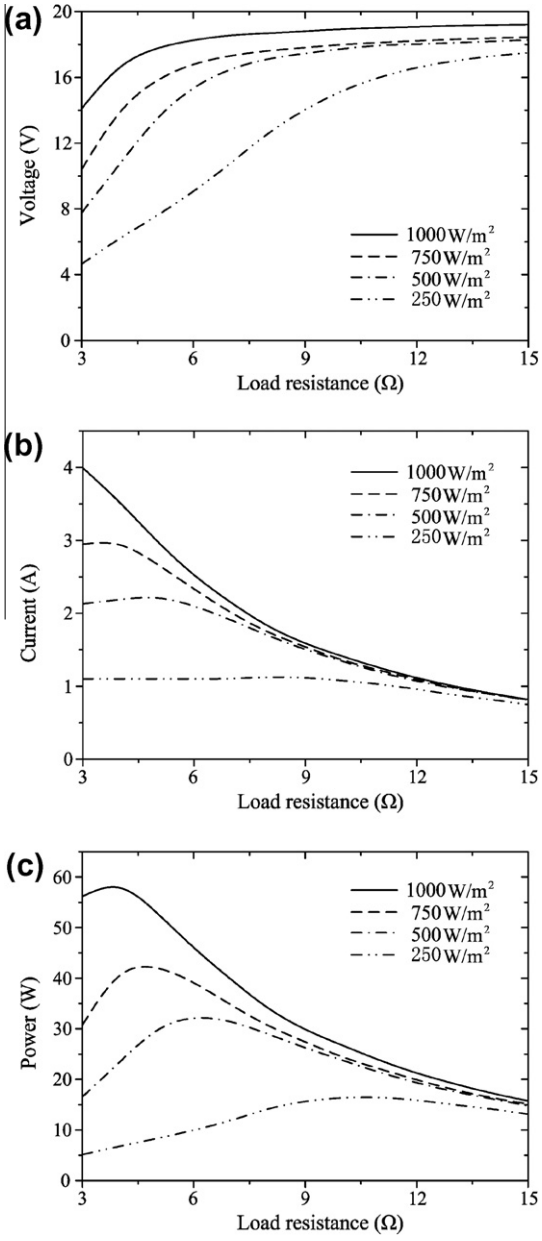

Fig. 10. Output characteristics versus load resistance of the PVG. (a) Output voltage. (b) Output current. (c) Output power.

4. Experimental results

Firstly, when the temperature of the cold-side of the TEG is kept at 50 °C, the output voltage, current, and power of the TEG at different hot-side temperatures, namely 100 °C, 150 °C, 200 °C, and 250 °C, are recorded by changing the load resistance from 3 Ω to 15 Ω as shown in Fig. 8. It can be found that the output characteristics vary non-linearly with the temperature and load. The corresponding maximum power and internal resistance at difference hot-side temperatures are summarized in Fig. 9. It can be found that the maximum power points of the TEG at different temperatures drift with the increment of output voltage.

Secondly, with the surface temperature of the PVG kept at 40 °C, the output voltage, current, and power of the PVG at different irradiances, namely 250 W/m^2, 500 W/m^2, 750 W/m^2 and 1000 W/m^2, are measured by changing the load resistance from 3 Ω to 15 Ω as shown in Fig. 10. It can be found that the output characteristics vary non-linearly with the irradiance and load. The maximum power and internal resistance at different insolation levels are summarized in Fig. 11. It can be found that the maximum power points of the PVG at different irradiances drift with the decrement of output voltage.

Considering the worst-case scenario of Eqs. (12) and (13) with the measured maximum power points from Figs. 9 and 11, the boundary of the battery voltage and duty cycles can be determined to ensure the system operating in the DCVM. The minimum acceptable duty cycles of the Ćuk–Ćuk MIC is 68.5% for the TEG branch, and 48.5% for the PVG branch. Then, the intermediate capacitors can be deduced by using (4) and (7). The main component values of the MIC are listed in Table 1, where the subscript $i = 1$ stands for the TEG branch, and $i = 2$ for the PVG branch.

The input resistances of the Ćuk–Ćuk MIC are shown in Fig. 12, in which the internal resistances of the TEG and PVG are also marked. When these two resistances match with each other, the maximum power point can be tracked. For verification, by tuning the duty cycle of each Ćuk circuit, the MPPT of each branch can be achieved as shown in Fig. 13. From Fig. 13a, it can be found that the duty cycle of the TEG branch for the MPPT decreases with the increase of temperature. It is expected because the higher the temperature difference, the higher the internal resistance of the TEG, the smaller the duty cycle is required to produce the matching

Table 1
Main component values of MIC.

	C_i (nF)	L_{1i} (mH)	L_{21} (μH)	C (μF)
TEG branch	91.1	1.6	220	1000
PVG branch	108.2	2.2		

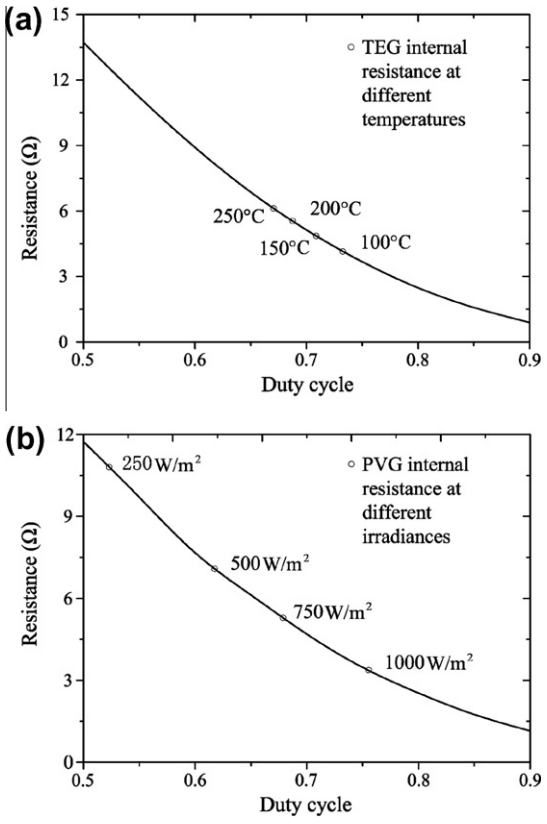

Fig. 12. Input resistances of the Ćuk–Ćuk MIC. (a) TEG branch. (b) PVG branch.

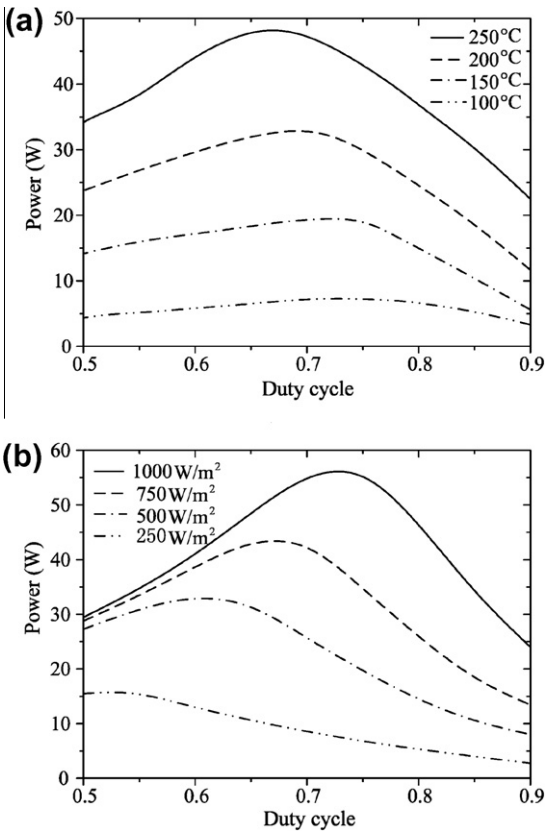

Fig. 13. Input powers of Ćuk branch versus duty cycle. (a) TEG branch. (b) PVG branch.

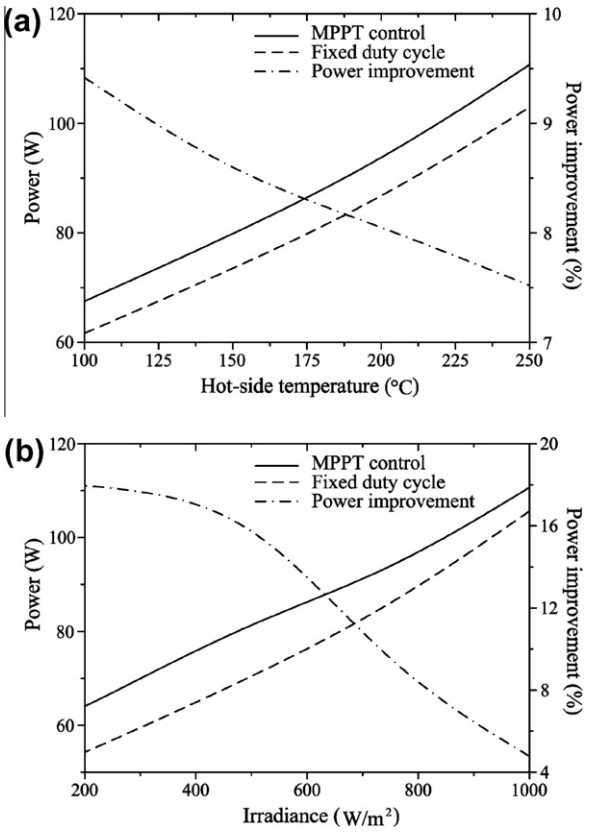

Fig. 14. Output power and power improvement. (a) With varying TEG output power. (b) With varying PVG output power.

input resistance of the Ćuk circuit. On the other hand, from Fig. 13b, it can be found that the duty cycle drift of the PVG branch for the MPPT is contrary. It is because the brighter the irradiance, the lower the internal resistance of the PVG is resulted.

In order to quantitatively assess the output power improvement due to the proposed MPPT, the TEG temperature is varied while the PVG output is kept at its maximum power point, and then the PVG irradiance is varied while the TEG output is kept at its maximum power point. Firstly, the output power is recorded when the hot-side temperature of the TEG is heated from 100 °C to 250 °C and the irradiance of the PVG is fixed at 1000 W/m^2. For the sake of comparison, the output power is also measured under the fixed duty cycle of 67%, which is close to the duty cycle of the maximum power point at 250 °C. As shown in Fig. 14a, the power improvement is from 7.5% to 9.4% due to the use of the MPPT. Secondly, the total output power is recorded when the irradiance of the PVG is controlled from 200 W/m^2 to 1000 W/m^2 and the hot-side temperature of the TEG is fixed at 250 °C. For the sake of comparison, the output power is also measured under the fixed duty cycle of 75%, which is close to the duty cycle of the maximum power point at 1000 W/m^2. As shown in Fig. 14b, the power improvement is from 4.8% to 17.9% resulting from the use of the MPPT. Therefore, the overall output power of the hybrid energy system can be significantly improved by the proposed Ćuk–Ćuk MIC using the MPPT.

5. Conclusions

In this paper, a new automotive TE–PV hybrid energy system has been proposed and implemented. Based on the proposed Ćuk–Ćuk MIC with the MPPT, both the TEG and PVG branches can achieve maximum power transfer independently. A 100 W prototype has been built and tested. The experimental results

successfully verify the validity of the proposed system. By scaling up the power ratings proportionally up to 1 kW, the proposed system will be very promising for different types of automobiles.

Acknowledgments

This work was supported and funded in part by the Matching Fund for NSFC Young Researcher Awards from the University Research Committee and a Grant (Project Code: 200807176032) from the Committee on Research and Conference Grants, The University of Hong Kong, Hong Kong Special Administrative Region, China.

References

[1] Chau KT, Chan CC. Emerging energy-efficient technologies for hybrid electric vehicles. Proc IEEE 2007;95(4):821–35.
[2] Preitl Z, Bauer P, Kulcsar B, Rizzo G, Bokor J. Control solutions for hybrid solar vehicle fuel consumption minimization. In: IEEE intelligent vehicle symposium; June 2007. p. 767–72.
[3] Yang J. Potential applications of thermoelectric waste heat recovery in the automotive industry. In: International conference on thermoelectrics; June 2005. p. 155–9.
[4] Duparchy A, Leduc P, Bourhis G, Ternel C. Heat recovery for next generation of hybrid vehicles: simulation and design of a Rankine cycle system. In: International electric vehicle symposium. Paper no. 3260191; May 2009.
[5] Yu C, Chau KT. Thermoelectric automotive waste heat energy recovery using maximum power point tracking. Energy Convers Manage 2009;50(6):1506–12.
[6] Zhang X, Chau KT, Chan CC. Overview of thermoelectric generation for hybrid vehicles. J Asian Electr Vehicles 2008;6(2):1119–24.
[7] Chau KT, Wong YS, Chan CC. An overview of energy sources for electric vehicles. Energy Convers Manage 1999;40(10):1021–39.
[8] Chau KT, Wong YS. Hybridization of energy sources in electric vehicles. Energy Convers Manage 2001;42(9):1059–69.
[9] Chau KT, Wong YS. Overview of power management in hybrid electric vehicles. Energy Convers Manage 2002;43(15):1953–68.
[10] Li YQ, Yu HY, Su B, Shang YH. Hybrid micropower source for wireless sensor network. IEEE Sens J 2008;8(6):678–81.
[11] Muhtaroglu A, Yokochi A, Jouanne A. A sustainable power architecture for mobile computing systems. J Power Sources 2008;178(1):467–75.
[12] Steinhuser A, Hille G, Kugele R, Roth W, Schulz W. Photovoltaic-hybrid power supply for radio network components. In: International telecommunications energy conference; June 1999. p. 1–9.
[13] Zhang X, Chau KT, Chan CC. Design and implementation of a thermoelectric–photovoltaic hybrid energy source for hybrid electric vehicles. In: International electric vehicle symposium. Paper no. 2130104; May 2009.
[14] Fairbanks J. Thermoelectric applications in vehicles status 2008. In: Europe conference on thermoelectrics; July 2008. p. 1–8.
[15] LaGrandeur J, Crane D, Eder A. Vehicle fuel economy improvement through thermoelectric waste heat recovery. In: Diesel engine emission reduction conference; August 2005. p. 1–7.
[16] Smith K, Thornton M. Feasibility of thermoelectrics for waste heat recovery in hybrid vehicles. In: International electric vehicle symposium. Paper no. 266; December 2007.
[17] Kim RY, Lai JS. Aggregated modeling and control of a boost–buck cascade converter for maximum power point tracking of a thermoelectric generator. In: Annual IEEE applied power electronics conference and exposition; February 2008. p. 1754–60.
[18] Liu YC, Chen YM. A systematic approach to synthesizing multi-input DC/DC converters. In: IEEE power electronics specialists conference; June 2007. p. 2626–32.